Pergamon

PII: S0191-8141(98)00042-X

Journal of Structural Geology, Vol. 20, No. 11, pp. 1495 to 1508, 1998

0191-8141/98 $ - see front matter

A revised model for the relationship between joint spacing and layer thickness

SHAOCHENG JI and KAZUKO SARUWATARI

Département de géologie, Université de Montréal, C.P. 6128, Succursale "Centre-Ville", Montréal, Québec, H3C 3J7, Canada. E-mail: jish@ere.umontreal.ca

(*Received* 5 *February* 1997; *accepted in revised form* 19 *March* 1998)

Abstract Hobbs' model [Hobbs, D. W. (1967) The formation of tension joints in sedimentary rocks: an explanation. *Geological Magazine* **104**, 550–556.] has been cited as one of the theories for interpretation of the linear relationship between saturated joint spacing (s) and bed thickness (t) in interbedded sedimentary rocks. However, this model is based on an assumption that the shear stress in the bounding non-jointing layers decreases linearly from the maximum value at the layer–matrix interface to zero at a distance exactly equal to the jointing layer thickness from the interface. We provide a revised analytical model which takes into account the non-linear decay of the shear stress and the effects of bounding bed thickness (d). The model shows that $s = \eta\sqrt{td}$ for the competent beds bounded by two incompetent layers nearly identical in thickness. The constant η depends on both material properties of rocks (i.e. the Young's modulus, tensile strength and fracture saturation strain of the competent bed, and the shear modulus of the incompetent layers) and decay modes of the shear stress in the bounding layers. If the ratio of d to t is constant, the relationship between s and t is linear. If d is constant, the joint spacing increases as a function of the square root of t. Complex t–d variations from Cambrian flysch sediments at Plage Victor in the Saint-Jean Port-Joli area of the Quebec Appalachians, however, result in a statistically linear relationship between s and t.

INTRODUCTION

Hobbs (1967) introduced for the first time to geologists the shear-lag model of Cox (1952) and modified the mathematical derivations of the model to incorporate an elastic layer–matrix system. As described by Gross *et al.* (1995), Hobbs' paper has been commonly cited as a theoretical explanation for the linear relationship between joint spacing and bed thickness in sedimentary rocks (Price, 1966; McQuillan, 1973; Ladeira and Price, 1981; Huang and Angelier, 1989; Narr and Suppe, 1991; Gross, 1993; Gross *et al.*, 1995; Wu and Pollard, 1995). However, Hobbs' model is based on an assumption that the shear stress in the matrix (bounding non-jointing beds), which is caused by the strain incompatibility between the competent layer and the incompetent matrix, decreases *linearly* from the maximum value at the layer–matrix interface to zero *at a distance exactly equal to the jointing layer thickness* from the interface [his equation (9)]. This assumption obliges a condition that must be met formally for Hobbs' model to apply: the incompetent layer thickness should be always larger than the jointing competent layer thickness (Narr and Suppe, 1991). In many sedimentary rocks, however, the bounding non-jointing beds are thin relative to jointed layer thickness (Narr and Suppe, 1991; Gross *et al.*, 1995). Moreover, finite-element analyses of Fischer *et al.* (1995) demonstrate that the shear stress formed by the strain incompatibility decays non-linearly in the matrix with the vertical distance from the layer–matrix interfaces. Theoretical analyses of the composites with an identical arrangement of constituents (Zhao and Ji, 1997) suggest that the shear stress should decrease from the maximum value at the layer–matrix interface to zero at half way between two neighboring competent layers. The reason is simple: the layer–matrix composite is considered as an edifice constructed from the identical 'unit-cell' building blocks. The boundary between two neighboring unit-cells should be a plane over which no shear stress acts because the composite is assumed to be applied to a uniform extension.

As noted by Gross *et al.* (1995), it is often difficult to understand the above problems in Hobbs' paper because it is compact and lacks illustrations. It is the purpose of this paper to provide a straightforward yet rigorous modification of the original Hobbs' shear-lag analysis so as to account for the non-linear decay of shear stress in the matrix. Starting from first principles and using equilibrium and continuity conditions, a revised model is provided for the relationship between joint spacing and bed thickness.

THE REVISED MODEL

Hobbs (1967) treated bedded strata as a lamellar composite containing continuous, aligned competent (higher elastic modulus) and incompetent (lower elastic modulus) layers of equal length (Fig. 1a). He assumed that each component behaves in a purely linear-elastic manner, that is, no plastic yielding is allowed. Further, in his treatment, residual stress effects are also neglected. If a uniform extensional strain (ε) is applied in the direction parallel to the layers (Fig. 1b), the resulting tensile stress will be higher in the competent layer

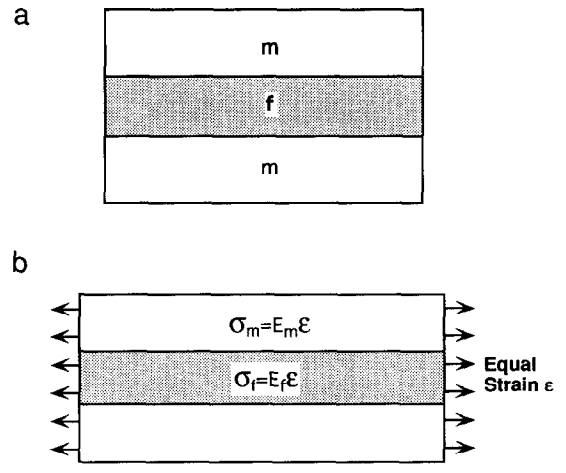

Fig. 1. Schematic illustrations of a lamellar composite containing continuous, aligned competent (f) and incompetent (m) layers of equal length. (a) The unstrained state. (b) The composite is subjected to a uniform, layer-parallel extensional strain (ε). In this case, the competent layer carried a greater stress than the incompetent layer.

than in the incompetent layers (matrix). Joints will then form in the competent layer at its weak points where the tensile stress has reached its critical tensile strength (C_0). The joints terminate at contacts with adjacent incompetent layers because the competent layer fails at much lower magnitudes of extensional strain than the incompetent layers (Garrett and Bailey, 1977).

Because joints are free surfaces across which no stress can be transferred (Lachenbruch, 1961; Pollard and Segall, 1987), the far-field extensional strain cannot be directly applied to a discontinuous, jointed layer segment (ACDB in Fig. 2a) from its ends (AB and CD planes in Fig. 2a). Thus, the tensile stress build-up in this layer segment is purely due to the stress transfer from the matrix to the competent layer by means of interfacial shear stresses. Because the interfaces between the layers (AC and BD in Fig. 2a) are assumed to be welded, the different amounts of layer-parallel displacements between the matrix and competent layer result in shear strains, and thus shear stresses, parallel to the layers. It is of considerable interest to know how tensile stress is built up in an individual layer segment because the final joint spacing is controlled by the magnitude and distribution of the stress. The stress transfer can be analyzed according to shear-lag model (Cox, 1952; Holister and Thomas, 1966; Kelly and MacMillan, 1986; Zhao and Ji, 1997). The following analysis does not address the problems of joint propagation and thus we are justified in ignoring the three-dimensional aspects of the phenomenon.

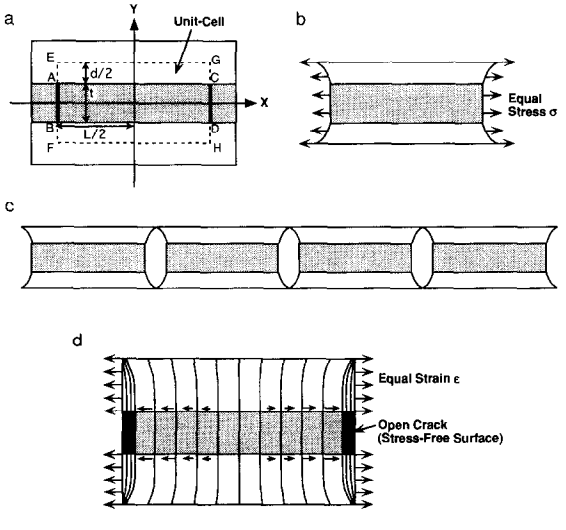

Fig. 2. Schematic illustration of a unit-cell (a) used in the mechanical equilibrium analysis of the shear-lag model for the layer–matrix system. Variables are defined in text. The coordinate origin is located at the center of the layer segment. The Z-axis is perpendicular to the X- and Y-axes. Under a uniform stress, the two ends of the unit-cell will be bent (b). As a result, a 'lens'-shaped void will be formed between two adjacent unit-cells (c). (d) shows the variation of the longitudinal displacements introduced on applying a uniform extensional strain at the ends of the matrix. The openings at joints are exaggerated.

In order to perform the shear-lag analysis, a unit cell is used. In the unit cell shown in Fig. 2(a), a jointed competent layer segment (ACDB) lies between two half incompetent beds (EGCA and BDHF), with joints (AB and CD) forming the ends of the competent layer segment. As suggested by Price (1966), a sedimentary bed always contains some randomly positioned pre-existing joints which can result from a Poisson process. The boundary conditions at the ends of the unit cell are critical for the analysis. First, the jointing layer is extended parallel to the X-direction and the tensile stress in this direction should be zero across each joint surface (AB and CD planes). Second, the interfaces between the layers are assumed to be welded and thus there is no interfacial slip. Third, the external loading on the ends of the matrix (EA, BF, GC and DH planes in Fig. 2a) cannot be uniform. If the loading is uniform, the edges of the matrix will be bent (Fig. 2b) during the deformation, and consequently, a 'lens'-shaped void will be formed between two adjacent unit-cells (Fig. 2c). Such a scenario implies that the joint is extended from the competent layer into the neighboring incompetent beds a distance equal to half thickness of the incompetent beds. In nature, however, the joints are restricted to the competent layers (Huang and Angelier, 1989; Narr and Suppe, 1991; Gross *et al.*, 1995). In order to avoid the above problem, we assume that the ends of the matrix experience a uniform extensional strain (ε) and the existing joints at the ends of the competent layer segment are open during the deformation (Fig. 2d). This assumption implies that two adjacent competent layer segments are separated to some distance during the extension. However, the exact size of the gaps is not critical in this model. The model shown in Fig. 2(d) is believed to represent sufficiently well for our purpose the state of affairs around a jointed layer segment.

In the following analyses, we use the shear-lag model developed by Cox (1952) and summarized by Holister and Thomas (1966), Kelly and MacMillan

(1986), and Zhao and Ji (1997). This model is elegant in its simplicity and provides accurate estimates of the longitudinal tensile stress in the continuous or discontinuous fibers embedded in the weak matrix. Hence the model has been widely used by geologists to explain the origin of extension fracture boudinage (Lloyd *et al.*, 1982; Masuda and Kuriyama, 1988; Ji and Zhao, 1993; Ji *et al.*, 1997; Ji, 1997). The model is also able to provide the distribution of shear stresses in the weak matrix surrounding the strong inclusions and accordingly interpret the variations of dislocation density and of recrystallized grain size in composites and polyphase rocks (Dunand and Mortensen, 1991; Zhao and Ji, 1997). Furthermore, the model predicts the elastic or flow strength of two-phase composites (e.g. Nardone and Prewo, 1986; Zhao and Ji, 1993) and rocks (Ji and Zhao, 1994).

Under the above conditions, as shown in detail in the shear-lag model (Hobbs, 1967; Kelly and MacMillan, 1986; Lloyd *et al.*, 1982), the governing equation for the tensile stress in the competent layer segment, $\sigma_f(x)$, is given by

$$\sigma_f(x) = E_f\varepsilon + \frac{S_1}{A_f}\sinh(\beta x) + \frac{S_2}{A_f}\cosh(\beta x) \tag{1}$$

where ε is the far-field strain, E_f and A_f are the Young's modulus and the area of cross-section of the competent layer, respectively. $A_f = bt$, where t and b are the thickness and width of the competent layer in the Y- and Z-directions (Fig. 2a), respectively.

$$\beta = \left(\frac{H}{E_f A_f}\right)^{1/2} \tag{2}$$

where H is a constant, depending on the geometrical arrangement of the layer and the matrix and on their respective elastic moduli.

In equation (1), S_1 and S_2 are constants which can be determined according to the following boundary conditions:

$$\sigma_f\left(-\frac{L}{2}\right) = \sigma_f\left(\frac{L}{2}\right) = 0 \tag{3}$$

where L is the length of the layer segment (Fig. 2a). Equation (3) is due to the fact that the tensile stress is reduced to zero at the existing joints since they are free surfaces (Lachenbruch, 1961; Pollard and Segall, 1987).

Substituting equation (1) into equation (3), we obtain

$$S_1 = 0 \tag{4}$$

and

$$S_2 = -\frac{E_f A_f \varepsilon}{\cosh\left(\frac{\beta L}{2}\right)}. \tag{5}$$

The distribution of tensile stress in the competent layer segment is then:

$$\sigma_f(x) = E_f\varepsilon\left(1 - \frac{\cosh(\beta x)}{\cosh\left(\frac{\beta L}{2}\right)}\right) \tag{6}$$

where equation (6) shows that the tensile stress in a competent layer segment builds up from the ends ($x = -L/2$ and $x = L/2$) and is a maximum at the center (Fig. 3).

The value of H can be obtained from the following analysis. If $P(x)$ is the load in the competent layer segment at a distance x from the origin of coordinates (Fig. 2a), Cox (1952) assumed

$$\frac{dP(x)}{dx} = H[u(x) - v(x)] \tag{7}$$

where $u(x)$ is the longitudinal displacement in the competent layer and $v(x)$ is the corresponding displacement the matrix would undergo if the competent layer were absent (Hobbs, 1967; Kelly and MacMillan, 1986; Lloyd *et al.*, 1982).

If $\tau(x, y)$ is the shear stress, in the x direction, on planes parallel to the XZ plane (Fig. 2a), then at the interface between the layer and the matrix, the shear stress is $\tau(x, t/2)$. According to mechanical equilibrium,

$$dP(x) = -2\tau(x, t/2) \cdot (b\,dx) \tag{8}$$

or

$$\frac{dP(x)}{dx} = -2b\tau(x, t/2) = H[u(x) - v(x)] \tag{9}$$

Therefore,

$$H = -\frac{2b\tau(x, t/2)}{u(x) - v(x)}. \tag{10}$$

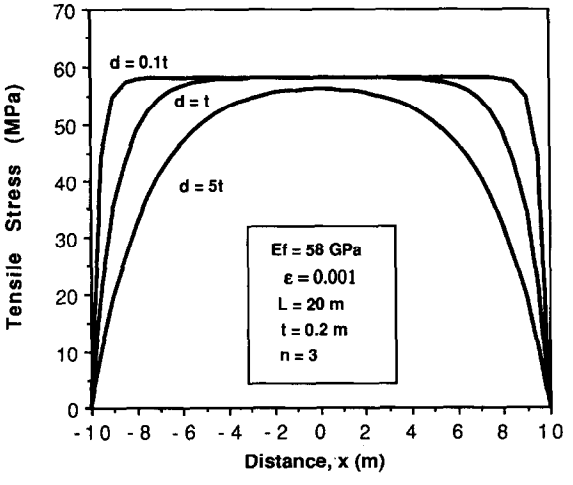

Fig. 3. Predicted tensile stress variations, as functions of the incompetent layer thickness ($d = 0.1t$, $d = t$, and $d = 5t$), along a competent layer ($t = 0.2$ m and $L = 20$ m). Using $E_f = 58$ GPa, $E_f/E_m = 3$, $\varepsilon = 0.1\%$, $\nu_m = 0.25$, and $n = 3$ as input data.

From the mechanical equilibrium point of view (Zhao and Ji, 1997), the shear stress formed by the strain incompatibility between the layer and the matrix should progressively decrease in the Y direction from the maximum value [$\tau(x, t/2)$] at the layer/matrix interface to zero at the middle way between two neighboring competent layers (EG and FH planes in Fig. 2a), that is,

$$\tau(x, y) = 0, \text{ when } y = \frac{t+d}{2} \tag{11}$$

and

$$\tau(x, y) = \tau(x, t/2), \text{ when } y = \frac{t}{2}. \tag{12}$$

The reason for this is that the boundaries of the unit cell (EG and FH planes in Fig. 2a) should have zero shear stress. Lloyd *et al.* (1982) assumed that shear stress is constant in the X direction on any XZ plane parallel to the layer [their equation (10)]. However, their assumption cannot satisfy the above mechanical equilibrium conditions (Zhao and Ji, 1997).

Hobbs (1967) proposed that the shear stress decreases in the Y direction in the matrix according to the following equation:

$$\tau(x, y) = \tau(x, y)|_{y=t/2}\left(\frac{t-y}{t}\right) \tag{13a}$$

He located the coordinate origin at the layer/matrix interface [his equation (9)]. If we locate the coordinate origin at the layer center (Fig. 2a), equation (13a) becomes

$$\tau(x, y) = \tau(x, y)|_{y=t/2}\left(\frac{\frac{3t}{2}-y}{t}\right). \tag{13b}$$

This assumption indicates that the shear stress in the matrix decreases linearly from the maximum value $\tau(x, y)|_{y=t/2}$ at the layer–matrix interface to zero at a distance exactly equal to the competent layer thickness (t) from the interface. Such a shear stress distribution does not apply to the case where $d < t$ (Fig. 2a) since the mechanical equilibrium cannot be attained. In nature, however, many non-jointing incompetent beds are much thinner than jointed beds. This situation is thus precluded by Hobbs' model. The above shortcomings in the Hobbs' model were also recognized by Narr and Suppe (1991), Gross *et al.* (1995) and Fischer *et al.* (1995).

Tyson and Davies (1965) performed a photoelastic study of the shear stresses in a quasi-infinite matrix (composed of araldite CT 200) around a single cylindrical fiber composed of the material dural. They found that the shear stresses in the matrix (τ_m) fall off radially approximately as the inverse of the distance (r) from the fiber axis. Namely, $\tau_m = \tau_i(r_f/r)$, where τ_i is the interfacial shear stress and r_f is the fiber radius. In the composites with large fiber volume fractions, however, the above equation is inappropriate to describe the shear stress distribution in the matrix. The reason is that the shear stress should be equal to zero at half way between two neighboring fibers (Zhao and Ji, 1997).

In contrast to Hobbs' assumption shown by equation (13a or b), two-dimensional finite element numerical simulations of Fischer *et al.* (1995) demonstrated that the bedding-parallel shear stress decreases non-linearly with increasing the vertical distance from the maximum value at the bedding interface to zero away from the interface.

A simple expression for the non-linear variations of $\tau(x,y)$, which can satisfy the boundary conditions given by equations (11) and (12), is the following:

$$\tau(x, y) = \tau(x, y)|_{y=t/2}\left(\frac{d+t-2y}{d-t+2y}\right)^n \tag{14}$$

where n is a decay constant larger than or equal to 1. As shown in Fig. 4, the shear stress decreases more rapidly with the vertical distance from the interface for larger n values. Although equation (14) is certainly not a unique solution to the boundary conditions, we could find no constraints for values of $\tau(x,y)$ from $y = t/2$ to $y = (t + d)/2$ to warrant the use of a more complicated function for $\tau(x, y)$. The actual decay model of the shear stress in the matrix affects the relationship between the joint spacing and bed thickness. We hope that our work will encourage experimental studies of the shear stress distribution and magnitude in the matrix. For simplicity, in the present study, we assume that the shear stress in the matrix can be described by equation (14).

Now let w be the displacement in the soft matrix due to the extension. If there is no slippage between the competent and incompetent layers, $w = u$. At a distance from the X-axis equal to $(t + d)/2$, we have $w = v$. Considering equation (14), we have the shear

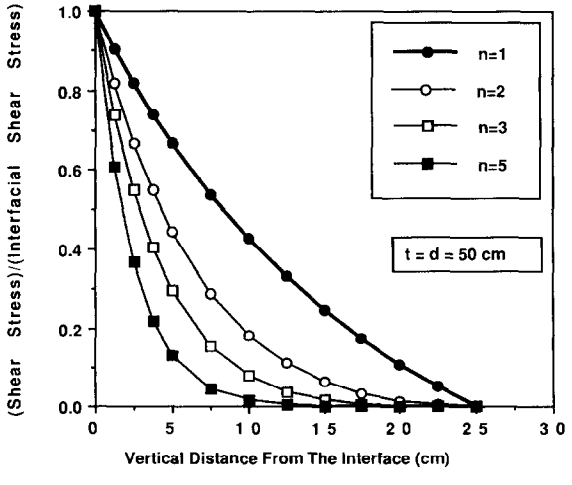

Fig. 4. Variations in the ratio of the matrix shear stress to the interfacial shear stress as a function of the vertical distance from the layer matrix interface. Calculated according to equation (14). $t = d = 50$ cm. The quantity n is the decay constant.

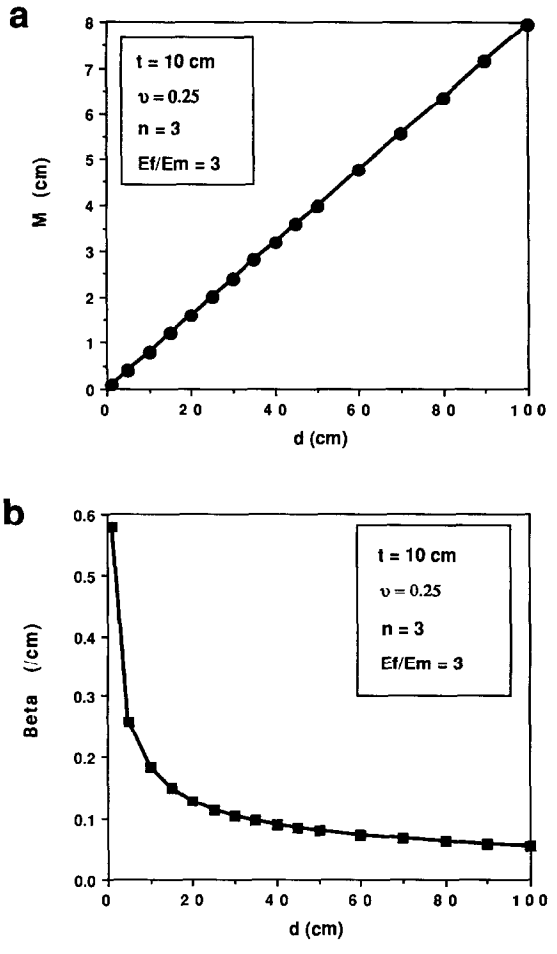

Fig. 5. (a) The linear variation of M-value and (b) the non-linear variation of β-value as a function of d. Calculated using $t = 10$ cm, $\nu_m = 0.25$, $n = 3$, and $E_f/E_m = 3$.

strain in the matrix described by the following equation:

$$\frac{\partial w}{\partial y} = \frac{\tau(x, y)}{G_m} = \frac{\tau(x, t/2)}{G_m}\left(\frac{d + t - 2y}{d - t + 2y}\right)^n \tag{15}$$

where G_m is the shear modulus of the incompetent matrix. Integrating from $t/2$ to $(t + d)/2$, thus

$$v - u = \Delta w = \int_{t/2}^{(t+d)/2} \frac{dw}{dy}dy = \frac{\tau(x, t/2)M}{G_m} \tag{16}$$

where

$$M = \int_{t/2}^{(t+d)/2}\left(\frac{d + t - 2y}{d - t + 2y}\right)^n dy. \tag{17}$$

Equation (17) requires numerical methods for its solution. For a given n value, the M-value increases with the thickness of incompetent layer (d) in an approximately linear manner (Fig. 5a). The M-value is independent of t.

Substituting equation (16) into equation (10), we have

$$H = \frac{2bG_m}{M}. \tag{18}$$

Then, substituting equation (18) into equation (2), we obtain

$$\beta = \left(\frac{2bG_m}{E_f A_f M}\right)^{1/2} = \left[(1 + \nu_m)tM\frac{E_f}{E_m}\right]^{-1/2} \tag{19}$$

where ν_m is the Poisson ratio of the incompetent layer, and E_f/E_m is the elastic contrast between the competent and the incompetent layers. For a given competent layer, β value decreases non-linearly with increasing the d value (Fig. 5b).

From equations (1) and (9), we can obtain the shear stress at the layer/matrix interface ($y = t/2$):

$$\tau(x, t/2) = -\frac{1}{2b}\frac{dP(x)}{dx} = -\frac{A_f}{2b}\frac{d\sigma_f(x)}{dx} = \frac{t}{2}E_f\varepsilon\beta\frac{\sinh(\beta x)}{\cosh\left(\frac{\beta L}{2}\right)}. \tag{20}$$

The derivative $dP(x)/dx$ at each position along the layer length can be derived, in fact, from the slope of the stress transfer profile of Fig. 3. Figure 6 shows the variation along a layer of the shear stress at the layer–matrix interface $\tau(x, t/2)$. As expected by equation (20), the interfacial shear stress takes up maximum values at the ends of the jointed layer and sharply decays to zero at a distance which is termed 'the transfer length' in composite mechanics (Jahankhani and Galiotis, 1991). As shown in Fig. 6, the transfer length increases with increasing the ratio of d/t. The distribution of the interfacial shear stress in fiber composites has been experimentally measured employing Raman spectroscopy (Jahankhani and Galiotis, 1991) and photoelastic technique (Dow, 1961; Tyson and Davies, 1965). Their measured stress distribution patterns are very similar to our calculated results shown in Fig. 6.

According to equation (6), the maximum tensile stress in the competent layer occurs midway between two existing joints (i.e. $x = 0$), and is given by

$$(\sigma_f)_{max} = E_f\varepsilon\left(1 - \frac{1}{\cosh\left(\frac{\beta L}{2}\right)}\right). \tag{21}$$

The maximum tensile stress decreases with decreasing the aspect ratio (L/t) of the fragmented layer and with increasing the thickness of incompetent layers (Fig. 3). In other words, the maximum tensile stress in the layers increases with increasing the volume fraction of the layers.

When the magnitude of the tensile stress (σ_f) transferred from the matrix reaches the tensile strength, C_0, of the brittle layer, a new joint forms midway between the existing joints, and tensile stress goes to zero at this point. The joints are formed by a sequential process (Price, 1966; Hobbs, 1967; Narr and Suppe, 1991; Gross, 1993). After breakage, the segments are newly loaded in the course of extension and break again. Each segment has one maximum tensile stress along

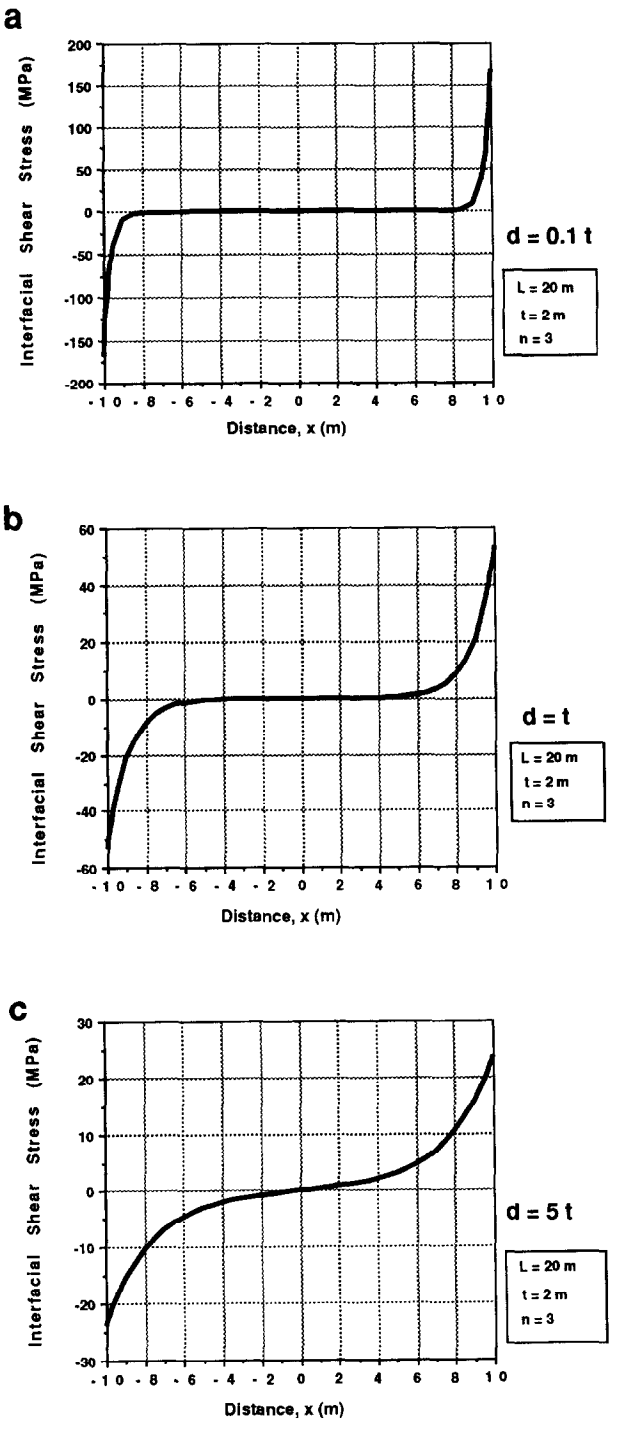

Fig. 6. Predicted variations along a competent layer (t = 2 m, L = 20 m) of the shear stress at the layer matrix interface as a function of the bounding bed thickness (d) according to equation (20). Using $E_f/E_m = 3$, $\nu_m = 0.25$, and $\varepsilon = 0.1\%$. (a) $d = 0.1t$, (b) $d = t$, and (c) $d = 5t$.

the loading direction, thus the fractured segment should be never broken along more than one plane at the same time if this segment is mechanically homogeneous. In sedimentary rocks, a number of parallel tensile joints occur in each single competent layer. These joints belong to different generations which were formed by a successive jointing process.

Equation (21) indicates that the magnitude of the maximum tensile stress in a jointed layer segment decreases with decreasing its length–thickness ratio (L/t). The sequential jointing process will decrease the aspect ratio and in consequence will reduce the maximum tensile stress in the subsegment. In other words, layer segments which have high aspect ratios break first. In addition, when a layer segment is jointed during tension, its internal stress is relaxed, and the force carried by this segment may be transferred to the surrounding matrix and particularly neighboring layers.

The final joint spacing (s) is thus controlled by a critical length (with respect to the layer thickness) below which the maximum tensile stress cannot exceed the tensile fracture strength of the layer (C_0). This sort of development is exactly analogous to the behavior in extension of certain types of fiber-reinforced composites (Klipeel *et al.*, 1990; Melanitis *et al.*, 1992) and rocks (Hobbs, 1967; Lloyd *et al.*, 1982; Ji and Zhao, 1993; Ji *et al.*, 1997). By equalizing $(\sigma_f)_{max}$ to C_0, we obtain the critical length of the layer segment (L_c) through the following equation:

$$L_c = \frac{2}{\beta}\cosh^{-1}\left(\frac{E_f\varepsilon}{E_f\varepsilon - C_0}\right). \tag{22}$$

In fact, L_c is the shortest length of layer segment which can fracture because in shorter segments the tensile stress nowhere exceeds the tensile strength of the layer. Segments longer than L_c, however, will fracture again. The minimum length of the layer segment possible should be equal to $L_c/2$ because segments shorter than L_c cannot fracture further (Lloyd *et al.*, 1982). When all the layer segments finally have their lengths between $L_c/2$ and L_c, joint spacing stops evolving and remains constant with increasing strain. This is a state of fracture saturation (Cobbold, 1979; Rives *et al.*, 1992; Wu and Pollard, 1995).

At the state of fracture saturation, there is a range of layer segment lengths: $L_c/2 \le L_i \le L_c$, where L_i is the length of jointed layer segments. If the frequency distribution of fracture spacing is a normal distribution in the range from $L_c/2$ to L_c, we might expect the mean fracture spacing (equivalent to the median joint spacing in the present case), s, to be:

$$s = \frac{3}{4}L_c \tag{23}$$

(Ohsawa *et al.*, 1978). Substituting equation (22) into equation (23), we obtain

$$s = \frac{3}{2\beta}\cosh^{-1}\left(\frac{E_f\varepsilon}{E_f\varepsilon - C_0}\right). \tag{24}$$

Then substituting equation (19) into equation (24), we have

$$s = \frac{3}{2}\left[t(1+\nu_m)M\frac{E_f}{E_m}\right]^{\frac{1}{2}}\cosh^{-1}\left(\frac{E_f\varepsilon}{E_f\varepsilon - C_0}\right) \qquad (25)$$

where E_m and ν_m are the Young's modulus and the Poisson's ratio of the matrix, respectively. It is worth mentioning that Hobbs (1967) took L_c as s.

Equation (25) shows that the median joint spacing depends on the thickness of competent layer, the mechanical properties (E_f, E_m, ν_m and C_0) of both the competent and adjacent incompetent layers, and the degree of tectonic deformation (ε). It depends also on the thickness of incompetent layers (d) and the decay constant (n) of the shear stress in the incompetent layers because the M value in equation (25) is controlled by these two factors.

It should be pointed out that the applied strain (ε) in equation (25) cannot exceed the fracture saturation strain of the jointed layer. As shown by experiments of Rives *et al.* (1992) and Wu and Pollard (1992, 1995), when the applied strain reaches a critical value, fracture spacing stops evolving and remains nearly constant. The critical strain is called fracture saturation strain. In other words, joint spacing decreases with increasing strain before the fracture saturation strain is reached. In contrast, a greater applied strain beyond the fracture saturation strain will not significantly change the joint spacing (Cobbold, 1979; Narr, 1991; Narr and Suppe, 1991; Rives *et al.*, 1992; Wu and Pollard, 1992, 1995). Inputting the fracture saturation strain into equation (25), one can obtain the relationship between saturated joint spacing and bed thickness.

ANALYSIS OF FIELD DATA

Field data were collected from the St-Roch Formation of Lower Cambrian age in continuous exposures at Plage Victor along the Saint-Lawrence River near Saint-Jean–Port-Joli (Fig. 7) which is 113 km northeast of Quebec City. Rocks in this area belong to the flysch sequence belt which forms the western front of the Quebec Appalachians. The regional geology and stratigraphy of this area were given in Hubert (1967), St-Julien (1967), Hubert (1969) and Shalaby (1977).

The tectonic structures of the area are characterized by NE–SW-trending folds and reverse faults which formed during the Appalachian compression. In the study area ($900 \times 300\ m^2$), tectonic strain is fairly homogeneous except near the faults (Fig. 7). Joints are confined to the hard sandstone, siltstone and limestone layers while the soft shale and mudstone layers remain non-jointed (Fig. 8). The joints are approximately planar fractures with little or no offset parallel to the fracture plane, and thus extension fractures ('mode I' cracks of fracture mechanics) which formed as the result of extensional strain normal to the plane of fracture (Pollard and Aydin, 1988). There are two sets of joints, one strikes about 325–340° and dips between 65° and 85°, and the other trends about 140–155° and dips 10–30°. Only the first set of joints were measured in the field because they are nearly perpendicular to fold axes and likely to have been formed by a regional tectonic extension induced by the Appalachian compression. The joint spacing of this set in thick beds commonly is greater than in thin beds, as shown in Fig. 8. Measurements were performed on the jointed layers (i) having a uniform thickness; (ii) bounded by two incompetent layers nearly identical in thickness; (iii) not disturbed by faults; and (iv) having at least 40 parallel joints whose spacing could be measured on the continuous outcrop. In total, 42 sandstone layers were measured, among them 30 from area H, 5 from area J and 7 from area K (Fig. 7). Small numbers of measurements from areas J and K make it impossible to investigate the effect of strain on joint spacing.

Plume structures and rib marks on joint surfaces in uniform fine-grained siltstones and limestones indicate that the joints initiated and propagated away from point defects such as nodules, pebbles, pores, and minerals (Price, 1966; Syme-Gash, 1971; Bahat and Engelder, 1984). It may be reasonable to assume that such defects are randomly distributed in the rocks.

The joint-spacings belonging to a single joint set along an individual bed with a uniform thickness generally display an appearance of normal distribution (Fig. 9a,c) and occasionally positively skewed frequency distribution (Fig. 9b). Similar skewed distributions have been described as gamma distributions (Huang and Angelier, 1989; Gross, 1993; Castaing *et al.*, 1996) or log-normal distributions (Sen and Kazi, 1984; Narr and Suppe, 1991; Rives *et al.*, 1992; Becker and Gross, 1996; Pascal *et al.*, 1997). Huang and Angelier (1989) suggest that the skewed distributions are due to censuring of the minute joints, which do not cut completely the competent layer, during measurements. Their suggestion is based on a fact that there are several different orders of spacing of joints in rocks in which only the larger orders are visible as joints (e.g. Castaing *et al.*, 1996). Narr and Suppe (1991) and Becker and Gross (1996) propose that such distributions are a direct consequence of the stress reduction shadow, which inhibits formation of new joints in the vicinity of existing joints. Rives *et al.* (1992) suggest that joint set development is controlled by the spatial distribution of initiation points, the size of the interaction zones, the initiation and propagation criteria of the joint set, and the stage of evolution. The evolution from a negative exponential to a normal distribution through a log-normal distribution corresponds to an increase in degree of fracture saturation with increasing extension strain. If this is true, we infer that the normal distribution of joint spacing, observed in this study, indicates a state of fracture saturation

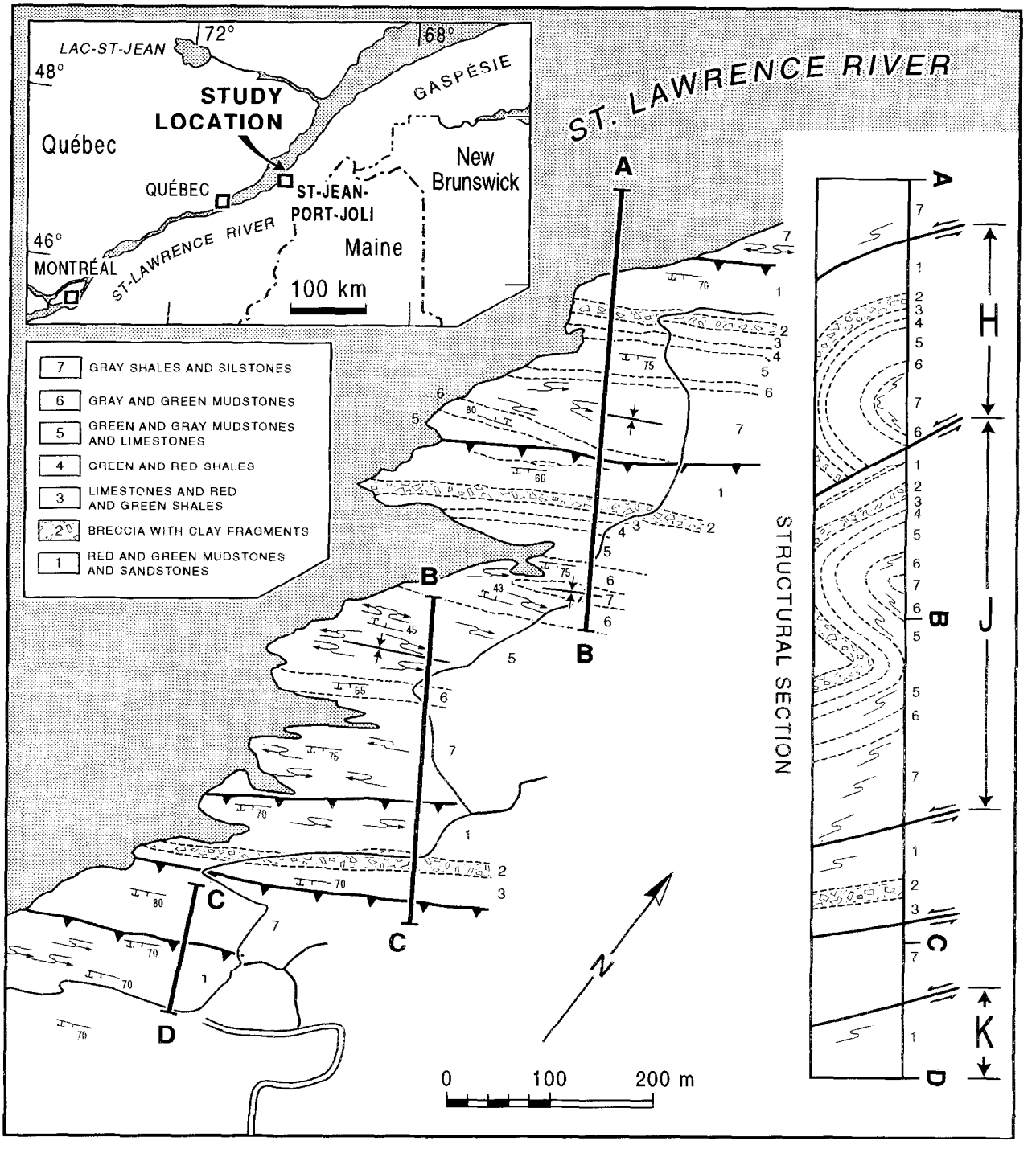

Fig. 7. Geological map of Plage Victor along the Saint-Lawrence River near Saint-Jean-Port-Joli, Quebec. Modified from Hubert (1969). Seven subunits were divided by Hubert (1969) and Shalaby (1977). Subunit 1 is characterized by interbedded structures of siltstones, sandstones and red and green mudstones. Subunit 2 is a slump deposit with irregular mudstone breccia, flow rolls and irregular fabrics of fold axes. Subunit 3 consists of limestone conglomerate and red and green shales. Subunit 4 is constituted of red and green shales with laminated calcareous siltstones. Subunit 5 is characterized by green and gray mudstones interbedded with thick laminated limestones and siltstones. Subunit 6 consists of interbedded limestones and gray and green mudstones. Subunit 7 consists of red and green mudstones and thin beds of sandstones. Lithology and thickness of the sandstone beds are persistent laterally. The joint data were measured mainly from subunits 1 and 7.

for the jointed layers. Thus the relationship between joint spacing and bed thickness may provide meaningful insights about the material properties of the rocks because the spacing is not sensitive to the applied strain at the stage of fracture saturation (Wu and Pollard, 1995).

Figure 10(a) shows plots of median joint spacing vs layer thickness for 42 studied sandstone layers. Each

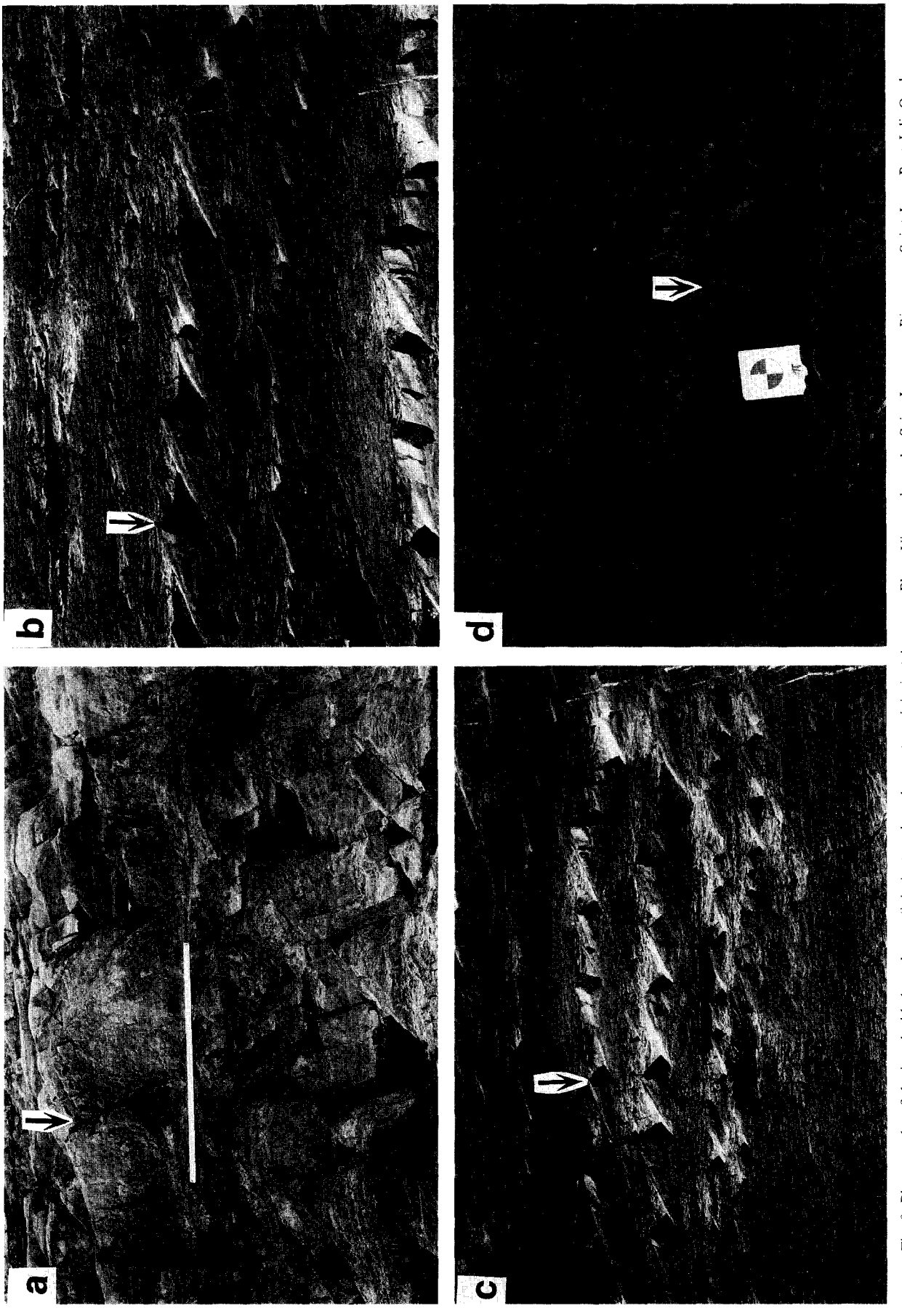

Fig. 8. Photographs of the interbedded sandstone (jointing) and mudstone (non-jointing) layers at Plage Victor along the Saint-Lawrence River near Saint-Jean-Port-Joli, Quebec. A single set of steeply dipping joints (indicated by arrow) was chosen for the present study. Note that the even joint spacing in thicker sandstone layers is regularly greater than in thinner beds.

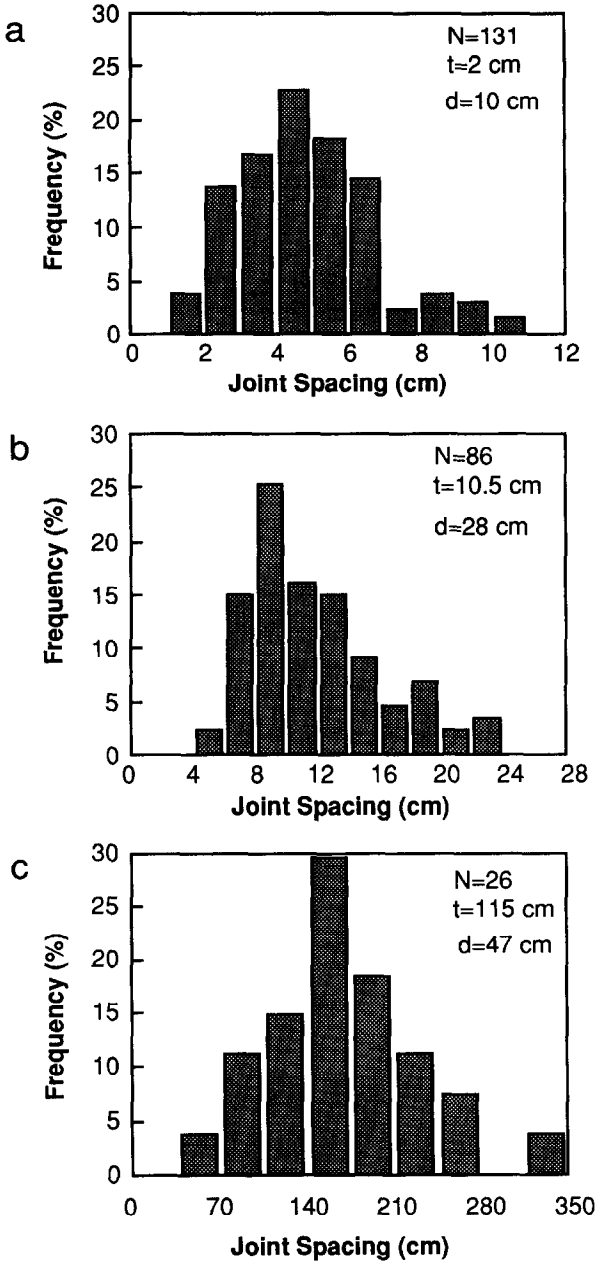

Fig. 9. Histograms for joint spacing values sampled in three typical sandstone layers at Plage Victor in the Saint-Jean–Port-Joli area of the Quebec Appalachians. N, number of measurements; t, thickness of layer; d, thickness of bounding non-jointed layers.

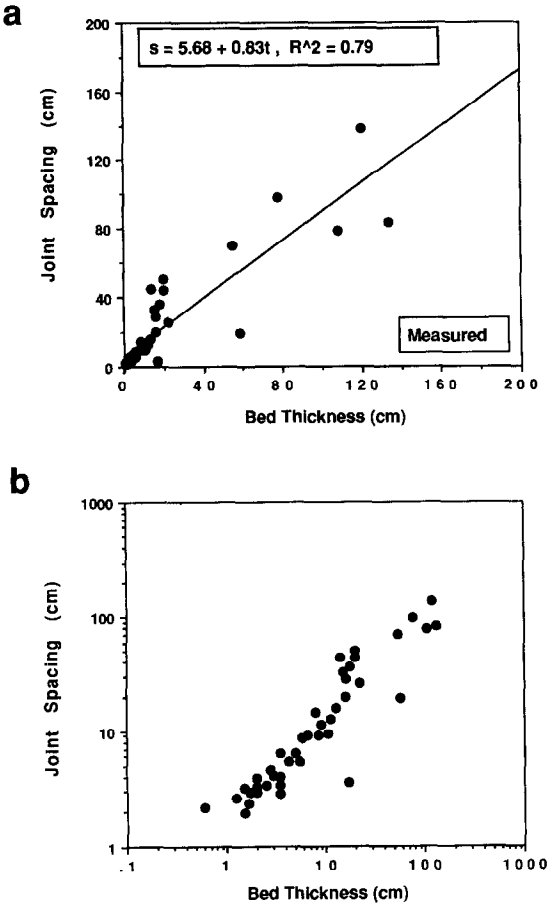

Fig. 10. Plots of median joint spacing (s) vs layer thickness of sandstone, measured from Plage Victor in the Saint-Jean–Port-Joli area of the Quebec Appalachians. (a) The data are represented in a linear scale so that the linear relationship between joint spacing and bed thickness may readily be seen. (b) The data are represented in a logarithmic scale in order to obviate the problem relating to the unresolvable data near the origin.

point in Fig. 10(a) is the median spacing of 40–250 measurements. The best-fit straight line for these data has a slope equal to 0.83 although there is considerable scatter in the data on spacing for $t > 20$ cm. Such a slope is referred to as the coefficient of joint spacing, K (Ladeira and Price, 1981). Table 1 lists the K-values of sandstones reported in the literature (Price, 1966; Angelier *et al.*, 1989; Aydan and Kawamoto, 1990; Narr and Suppe, 1991; Gross, 1993). These K-values vary from 0.60 to 1.27 with a mean value of 0.90. Our measured K-value from Saint-Jean–Port-Joli is close to the mean value for sandstones.

In order to calculate the theoretical joint spacing in the layers, we need the material constants E_f, E_m, ν_m, and C_0 in addition to the measured t and d values. In the present case, E_f and C_0 are the Young's modulus and tensile fracture strength of sandstone, respectively. For the shale and mudstone, we assume that $E_m = 16$ GPa (Gross *et al.*, 1995) and $\nu_m = 0.25$. For sandstone, $E_f = 58$ GPa, which is obtained by averaging all the Young's moduli calculated from P-wave velocities and densities of sandstones at 100 MPa (Christensen, 1989). Because the joints were formed at depth in the

Table 1. Coefficient of joint spacing (K), defined as the slope of the median joint spacing vs the layer thickness regression line, for sandstones

Lithology	K-value	References
Sandstone	1.27	Aydan and Kawamoto (1990)
Sandstone	1.20	Price (1960)
Porcelanite & Siliceous Shale	0.82	Narr and Suppe (1991)
Sandstone	0.60	Angelier *et al.* (1989)
Sandstone (Alegria)	0.81	Gross (1993)
Sandstone (Gaviota)	0.79	Gross (1993)
Sandstone	0.83	this study

crust, the Young's moduli measured at room pressure (Hatheway and Kiersch, 1989) were not used in our calculations. As done by Gross *et al.* (1995) and Fischer *et al.* (1995), we assumed that the fracture saturation strain is 5×10^{-4}/s. The decay constant (n) of the shear stress in the matrix is taken to be 3. As shown in Fig. 11, a good general similarity between the calculated and measured relationships between s and t is found using $C_0 = 20$ MPa. If the fracture saturation strain is taken to be 10^{-3}/s, an unrealistic C_0 value as high as 40 MPa is needed to achieve such a similarity.

DISCUSSION

There is a linear relationship between M and d, $M = jd$, where j is a constant. equation (25) can be written as

$$s = \eta\sqrt{td} \tag{26}$$

where

$$\eta = \frac{3}{2}\left[j(1+\nu_m)\frac{E_f}{E_m}\right]^{1/2} \cosh^{-1}\left(\frac{E_f\varepsilon}{E_f\varepsilon - C_0}\right). \tag{27}$$

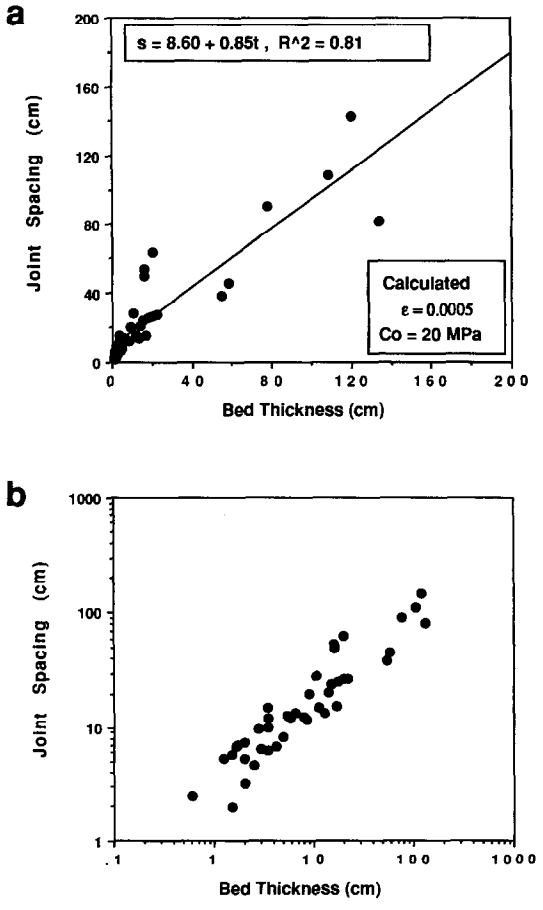

Fig. 11. Calculated joint spacings according to equation (25), using $E_f = 58$ GPa, $E_m = 16$ GPa, $\nu_m = 0.25$, $\varepsilon = 5 \times 10^{-4}$ s^{-1}, $C_0 = 20$ MPa, and t–d data from Fig. (13). (a) Linear scale. (b) Logarithmic scale.

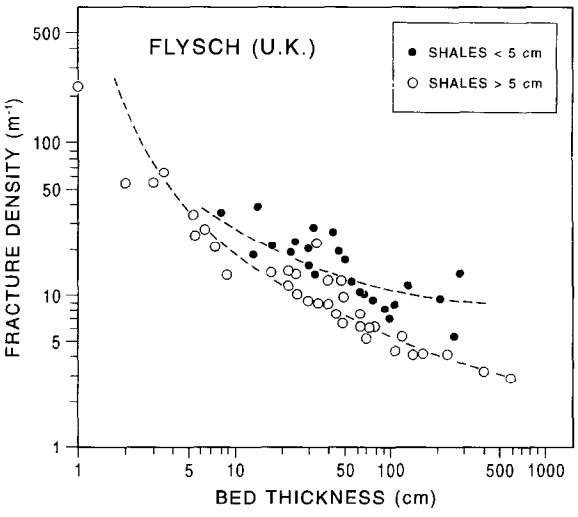

Fig. 12. Relationship between fracture density and competent bed thickness for different thickness of adjacent incompetent layers in the Carboniferous flysch of Devon and Cornwall (U.K.). The fracture density is defined as the number of fractures per meter. The fracture density in the competent layers which adjoin incompetent layers thicker than 5 cm is significantly smaller (for a given thickness of competent layer) than when the adjacent layers are thinner than 5 cm. After Ladeira and Price (1981)

The constant η depends on both material properties of rocks and decay modes of the shear stress in the bounding beds.

Equation (26) indicates that the joint spacing depends not only on the jointed layer thickness (t) but also on the non-jointed layer thickness (d). This agrees qualitatively with Ladeira and Price's (1981) field data collected in Carboniferous flysch exposed near Devon and Cornwall (U.K.). They found that the joint spacing in the competent layers which adjoin incompetent layers thicker than 5 cm is significantly larger (for a given thickness of competent layer) than when the adjacent layers are thinner than 5 cm (Fig. 12). Using finite-element techniques, Fischer *et al.* (1995) attempted to examine the effects of bounding bed thickness on the size of stress reduction shadow, and hence joint spacing. They demonstrated that the joint spacing first increases with increasing d/t (from 0.1 to 0.33), but then decreases with increasing d/t (from 0.33 to 0.66). They concluded that the observed variations are nonsystematic and primarily due to inaccuracies in their numerical solution and contouring algorithm.

Equation (26) shows that the relationship between joint spacing (s) and bed thickness (t) depends on the relationship between t and d. If the ratio of d to t is constant, the relationship between s and t is linear. That is to say, a linear relationship occurs between s and t when d varies linearly with t. Hobbs (1967) could obtain a linear relationship between s and t because he assumed that the shear stress in the matrix extends a distance exactly equal to t in the direction normal to the layer from the interface (i.e. he assumes that $d = 2t$). The well-documented linear relationship between s and t (< 1.0 m) in sedimentary sequences

(Price, 1966; McQuillan, 1973; Ladeira and Price, 1981; Aydan and Kawamoto, 1990; Narr and Suppe, 1991) may indicate a statistically linear relationship between the competent bed thickness and the incompetent layer thickness.

In other cases, equation (26) predicts a non-linear increase of the joint spacing (s) with bed thickness (t). For example, when d is constant or d t is constant, the joint spacing increases as a function of the square root of the bed thickness, that is, $s \propto \sqrt{t}$. Mandal *et al.* (1994) carried out a series of experiments using rigid layers of plaster of Paris with different thicknesses resting on a ductile substratum of pitch with a constant thickness. They observed that the joint spacing is proportional to the square root of the bed thickness. It is noted that there is an important difference between our theoretical model and their experimental model. In our model, the competent layer is confined and bonded on its top and bottom surfaces to the adjacent incompetent layers. In the model of Mandal *et al.* (1994), however, the competent layer is bonded only to the incompetent substratum and has a shear-stress-free top surface. In both cases, the competent layer is loaded through shear stresses at the layer–matrix interface. Analysis of equation (8) suggests that the different boundary conditions of two models affect only the η value but the relation $s \propto \sqrt{td}$ is still valid. A doubly-bonded layer should have a smaller η value and accordingly a smaller joint spacing than a layer with a free top surface. Therefore, the agreement between our theoretical prediction and the experimental results of Mandal *et al.* (1994) allows us to speculate that the non-linear relationship between s and t documented in beds thicker than 1.0 m (Ladeira and Price, 1981), may be due to a fact that the thickness of incompetent layers in these sequences does not increase with competent bed thickness and is much less than the competent bed thickness.

Similarly, the transition from linear to non-linear relationships with increasing competent bed thickness, reported by Ladeira and Price (1981), may be related to a change in relationship between d and t with increasing t. Therefore, the relationship between joint spacing and bed thickness cannot be understood without measurements of incompetent layer thickness. Unfortunately, no published field measurement data except those in the present paper are available on the s–t–d relationships. We hope that our work will encourage the systematic measurements of s, t and d in the field.

For the sandstones at Plage Victor, Saint-Jean–Port-Joli, the measured t d relationship is quite complex (Fig. 13). Surprisingly, such complex t–d variations result in a statistically linear relationship between t and s (Fig. 11a).

Our shear-lag model deals with the distribution of joints in sedimentary rocks comprising alternating competent and incompetent beds. Apparently, the model cannot be applied to massive rock units or igneous intrusions where joints were formed by mechanisms which are different from the stress transfer discussed above. Effects of residual stresses, bending, cooling and unloading should play a major role in building up tensile stresses for formation of fractures in the massive rocks.

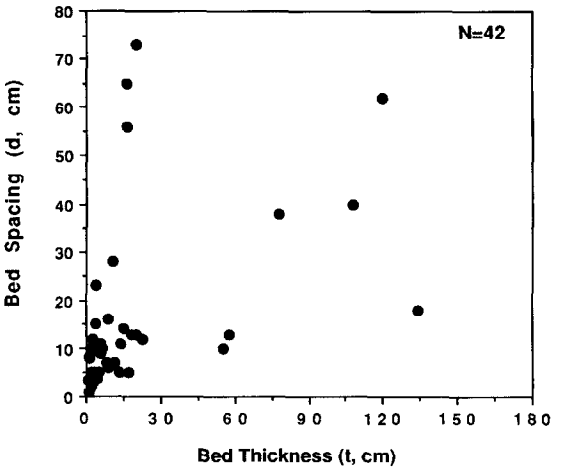

Fig. 13. Thicknesses of the sandstone and its bounding shale layers at 42 study sites from Page Victor in the Saint-Jean Port-Joli area of the Quebec Appalachians.

There are also a number of assumptions in our model, the elimination of which would lead to better correlation between model and observation.

1. Like other previous models (Price, 1966; Hobbs, 1967; Sowers, 1972; Narr and Suppe, 1991; Mandal *et al.*, 1994; Fischer *et al.*, 1995), the mechanical analysis is based on the assumption that there is no slip on the layer/matrix interfaces. Slip between the competent and incompetent layers will take place when the interfacial shear stress reaches the interfacial slip strength (τ_0). As shown by equation (20) and Fig. 6, the interfacial shear stress varies along the layer length and has a maximum at the layer ends and a minimum at the center of the layer. Therefore, the slip will occur over a certain length at each end of the layer. There is no interfacial slip for the center region of the layer. The tensile stresses for the slip and non-slip regions should be treated separately (Ji, 1997). The interfacial slip decreases the maximum tensile stress and thus increases the mean joint spacing.
2. It should be pointed out that the relationship between joint spacing and bed thickness depends on the actual mode of the shear stress decay in the matrix. The actual mode should be studied by well-designed experiments. Moreover, the decay constant (n) in equation (14) may also vary with the relative thickness of bounding layers with respect to jointed layer.
3. It has been assumed that the competent layer has a unique tensile strength whereas in a natural sedimentary bed, a fairly wide distribution of strengths

is expected (Narr and Suppe, 1991; Rives *et al.*, 1992) along the layer due to the random nature of defects (e.g. nodules, pebbles, pores, minerals and fossils).

4. The principal limitation to the theory presented in this paper is the assumption that the two incompetent layers bounding the jointed layer are of equal thickness. This arises from the simple form for the equation of mechanical equilibrium [i.e. equation (8)]. This assumption is also included in the previous models (Price, 1966; Hobbs, 1967; Narr and Suppe, 1991; Gross *et al.*, 1995; Fischer *et al.*, 1995). In order to remove this limitation, a complex unit-cell must be used and this cannot be treated with the present analytic solution. Nevertheless the analysis, we believe, has value for the bedded sedimentary rocks with nearly identical jointed layer spacings. A rigorous elastic analysis is possible at present by only numerical methods, but it may be too tedious to employ for each actual layer measured in the field.
5. The model is two-dimensional and implicitly assumes that joints are infinite in the third direction. Thus, the interaction between joints in this direction is ignored. Effects of the interaction on the frequency distribution of joint spacing have been discussed in Rives *et al.* (1992) and Wu and Pollard (1995).

The general trend of the field measurement results can be predicted by the model. It should be emphasized, however, that the prediction is based on the assumptions inherent in the model and on the selection of material constants (E_f, E_m, ν_m, C_0) and fracture saturation strain (ε) for the rocks. But we believe that the theoretical model will be a useful aid in analyzing the relationship between joint spacing and bed thickness.

Acknowledgements—We are indebted to Kathie St-Amand and Zheming Zhu for their assistance in the field. We thank Drs C. Castaing, J. P. Evans, M. R. Gross and H. Wu for critically reviewing the manuscript, and M. Demidoff for drawing Figs 7 and 12. This study was supported by grants from the NSERC research grants of Canada to S. Ji. This is LITHOPROBE contribution No. 915.

REFERENCES

Angelier, J., Souffache, B., Barrier, E., Bergerat, F., Bouaziz, S., Bouroz, C., Creuzot, G., Ouali, J. and Tricart, P. (1989) Distribution de joints de tension dans un banc rocheux: loi théorique et espacements. *Comptes Rendus de l'Academie des Sciences* **309,** 2119–2125.

Aydan, O. and Kawamoto, T. (1990) Discontinuities and their effect on rock mass. In *Rock Joints*, eds N. Barton and O. Stephansson, pp. 149–156. Balkema, Rotterdam.

Bahat, D. and Engelder, T. (1984) Surface morphology on cross-fold joints of the Appalachian plateau, New York and Pennsylvania. *Tectonophysics* **104,** 299–313.

Becker, A. and Gross, M. R. (1996) Mechanism for joint saturation in mechanically layered rocks—an example from southern Israel. *Tectonophysics* **257,** 223–237.

Castaing, C., Halawani, M. A., Gervais, F., Chilès, J. P., Genter, A., Bourgine, B., Ouillon, G., Brosse, J. M., Martin, P., Genna, A. and Janjou, D. (1996) Scaling relationships in intraplate fracture systems related to Red Sea rifting. *Tectonophysics* **261,** 291–314.

Christensen, N. I. (1989) Seismic velocities. In *Practical Handbook of Physical Properties of Rocks and Minerals*, ed. R. S. Carmichael, pp. 429–546. CRC Press, Boca Raton, Florida.

Cobbold, P. R. (1979) Origin of periodicity: saturation or propagation? *Journal of Structural Geology* **1,** 96.

Cox, H. L. (1952) The elasticity and strength of paper and other fibrous materials. *British Journal of Applied Physics* **3,** 72–79.

Dow, N. F. (1961) *General Electric Co., Space Mechanics Memo No. 102. May 1961.* Philadelphia, Pennsylvania.

Dunand, D. and Mortensen, A. (1991) Dislocation emission at fibers—I. Theory of longitudinal punching by thermal stresses. *Acta Metallurgica et Materialia* **39,** 1405–1416.

Fischer, M. P., Gross, M. R., Engelder, T. and Greenfield, R. J. (1995) Finite-element analysis of the stress distribution around a pressurized crack in a layered elastic medium: implications for the spacing of fluid-driven joints in bedded sedimentary rock. *Tectonophysics* **247,** 49–64.

Garrett, K. W. and Bailey, J. E. (1977) Multiple transverse fracture in 90° cross-ply laminates of a glass fiber-reinforced polyester. *Journal of Materials Science* **12,** 157–168.

Gross, M. R. (1993) The origin and spacing of cross joints: examples from the Monterey Formation, Santa Barbara Coastline, California. *Journal of Structural Geology* **15,** 737–751.

Gross, M. R., Fischer, M. P., Engelder, T. and Greenfield, R. J. (1995) Factors controlling joint spacing in interbedded sedimentary rocks: integrating numerical models with field observations from the Monterey Formation, USA. In *Fractography: Fracture Topography as a Tool in Fracture Mechanics and Stress Analysis*, ed. M. S. Ameen, pp. 215–253. Geological Society, London, Special Publication, **92.**

Hatheway, A. W. and Kiersch, G. A. (1989) Engineering properties of Rock. In *Practical Handbook of Physical Properties of Rocks*, ed. R. S. Carmichael, pp. 671–715. CRC Press, Boca Raton, Florida.

Hobbs, D. W. (1967) The formation of tension joints in sedimentary rocks: an explanation. *Geological Magazine* **104,** 550–556.

Holister, G. S. and Thomas, C. (1966) *Fiber-reinforced materials.* Elsevier, Amsterdam.

Huang, Q. and Angelier, J. (1989) Fracture spacing and its relation to bed thickness. *Geological Magazine* **126,** 355–362.

Hubert, C. (1967) Tectonics of part of the Sillery Formation in the Chaudiere–Matapedia segment of the Quebec Appalachians. *Royal Society of Canada Special Publication* **10,** 33–41.

Hubert, C. (1969) *Guidebook–Flysch Sedimentology in the Appalachians.* The Geological Association of Canada and The Mineralogical Association of Canada, Montreal.

Jahankhani, H. and Galiotis, C. (1991) Interfacial shear stress distribution in model composites, Part 1: A Kevlar 49 fiber in an epoxy matrix. *Journal of Composite Materials* **25,** 609–631.

Ji, S. (1997) Fracturing of garnet crystals in anisotropic metamorphic rocks during uplift: Reply. *Journal of Structural Geology* **19,** 1433–1435.

Ji, S. and Zhao, P. (1993) Location of tensile fracture within rigid-brittle inclusions in ductile flowing matrix. *Tectonophysics* **220,** 23–31.

Ji, S. and Zhao, P. (1994) Strength of two-phase rocks: a model based on fiber-loading theory. *Journal of Structural Geology* **16,** 253–262.

Ji, S., Zhao, P. and Saruwatari, K. (1997) Fracturing of garnet crystals in anisotropic metamorphic rocks during uplift. *Journal of Structural Geology* **19,** 603–620.

Kelly, A. and MacMillan, N. H. (1986) *Strong Solids.* Oxford Science Publications, Oxford.

Klipeel, Y. L., He, M. Y., McMeeking, R. M., Evans, A. G. and Mehrabian, R. (1990) The processing and mechanical behavior of an aluminum matrix composite reinforced with short fibers. *Acta Metallurgica et Materialia* **38,** 1063–1074.

Lachenbruch, A. H. (1961) Depth and spacing of tension cracks. *Journal of Geophysical Research* **66,** 4273–4292.

Ladeira, F. L. and Price, N. J. (1981) Relationship between fracture spacing and bed thickness. *Journal of Structural Geology* **3,** 179–183.

Lloyd, G. E., Ferguson, C. C. and Reading, K. (1982) A stress-transfer model for the development of extension fracture boudinage. *Journal of Structural Geology* **4,** 355–372.

Mandal, N., Deb, S. K. and Khan, D. (1994) Evidence for a non-linear relationship between fracture spacing and layer thickness. *Journal of Structural Geology* **16,** 1275–1281.

Masuda, T. and Kuriyama, M. (1988) Successive "mid-point" fracturing during microboudinage: an estimate of the stress–strain relation during a natural deformation. *Tectonophysics* **147,** 171–177.

McQuillan, H. (1973) Small-scale fracture density in Asmari formation of southwest Iran and its relation to bed thickness and structural setting. *The American Association of Petroleum Geologists Bulletin* **57,** 2367–2385.

Melanitis, N., Galiotis, C., Tetlow, P. L. and Davies, C. K. L. (1992) Interfacial shear stress distribution in model composites. Part 2: Fragmentation studies on carbon fiber/epoxy systems. *Journal of Composite Material* **26,** 574–610.

Nardone, V. C. and Prewo, K. M. (1986) On the strength of discontinuous silicon carbide reinforced aluminum composites. *Scripta Metallurgica et Materialia* **20,** 43–48.

Narr, W. (1991) Fracture density in the deep subsurface: techniques with application to Point Arguello oil field. *The American Association of Petroleum Geologists Bulletin* **75,** 1300–1323.

Narr, W. and Suppe, J. (1991) Joint spacing in sedimentary rocks. *Journal of Structural Geology* **13,** 1037–1048.

Ohsawa, T., Nakayana, A., Miwa, M. and Hasegawa, A. (1978) Temperature dependence of critical fiber length for glass fiber reinforced thermosetting resins. *Journal of Applied Polymer Science* **22,** 3203–3212.

Pascal, C., Angelier, J., Cacas, M.-C. and Hancock, P. L. (1997) Distribution of joints: probabilistic modelling and case study near Cardiff (Wales, U.K.). *Journal of Structural Geology* **19,** 1273–1284.

Pollard, D. D. and Aydin, A. (1988) Progress in understanding jointing over the past century. *Geological Society of America Bulletin* **100,** 1181–1204.

Pollard, D. D. and Segall, P. (1987) Theoretical displacements and stresses near fractures in rocks, with applications to faults, joints, veins, dikes, and solution surfaces. In *Fracture Mechanics of Rock*, ed. B. K. Atkinson. Academic Press, London, pp. 277–349.

Price, N. J. (1966) *Fault and joint development in brittle and semi-brittle rocks*. Pergamon Press, Oxford.

Rives, T., Razack, M., Petit, J.-P. and Rawnsley, K. D. (1992) Joint spacing: analogue and numerical simulations. *Journal of Structural Geology* **14,** 925–937.

Sen, Z. and Kazi, A. (1984) Discontinuity spacing and RQD estimates from finite length scanlines. *International Journal of Rock Mechanics and Mining Sciences and Geomechanics Abstracts* **21,** 203–212.

Shalaby, H. (1977) Analyse des Structures Geométriques et Interprétation Rhéologique d'un Slump Cambrien dans le Flysch de Saint-Jean Port-Joli, Appalaches du Québec. Thesis of M.Sc. Université de Montréal (Canada).

Sowers, G. M. (1972) Theory of spacing of extension fracture. *Engineering Geology Case Histories* **9,** 27–53.

St-Julien, P. (1967) Tectonics of part of the Appalachian region of southeastern Quebec. *Royal Society of Canada Special Publications* **10,** 41–47.

Syme-Gash, P. J. (1971) A study of surface features relating to brittle and semibrittle fracture. *Tectonophysics* **12,** 349–391.

Tyson, W. R. and Davies, G. J. (1965) A photoelastic study of the shear stresses associated with the transfer of stress during fiber reinforcement. *British Journal of Applied Physics* **16,** 199–205.

Wu, H. and Pollard, D. D. (1992) Propagation of a set of opening-mode fractures in layered brittle materials under uniaxial strain cycling. *Journal of Geophysical Research* **97,** 3381–3396.

Wu, H. and Pollard, D. D. (1995) An experimental study of the relationship between joint spacing and layer thickness. *Journal of Structural Geology* **17,** 887–905.

Zhao, P. and Ji, S. (1993) Comment on "Strengthening behavior of particulate reinforced MMCs" by Y. Wu and E. J. Lavernia, and "On the strength of discontinuous silicon carbide reinforced aluminum composites" by V. C. Nardone and K. M. Prewo. *Scripta Metallurgica et Materialia* **27,** 1443.

Zhao, P. and Ji, S. (1997) Refinements of shear-lag model and its applications. *Tectonophysics* **279,** 37–53.